



## Discrete wavelet transform analysis of surface electromyography for the fatigue assessment of neck and shoulder muscles

Suman Kanti Chowdhury, Ashish D. Nimbarte\*, Majid Jaridi, Robert C. Creese

Industrial and Management Systems Engineering, West Virginia University, PO Box 6070, Morgantown, WV 26506-6107, United States

### ARTICLE INFO

#### Article history:

Received 27 July 2012

Received in revised form 1 May 2013

Accepted 1 May 2013

#### Keywords:

Discrete wavelet transform

Fatigue

Neck

Shoulder

Dynamic repetitive exertions

Musculoskeletal disorders

### ABSTRACT

Assessment of neuromuscular fatigue is essential for early detection and prevention of risks associated with work-related musculoskeletal disorders. In recent years, discrete wavelet transform (DWT) of surface electromyography (SEMG) has been used to evaluate muscle fatigue, especially during dynamic contractions when the SEMG signal is non-stationary. However, its application to the assessment of work-related neck and shoulder muscle fatigue is not well established. Therefore, the purpose of this study was to establish DWT analysis as a suitable method to conduct quantitative assessment of neck and shoulder muscle fatigue under dynamic repetitive conditions. Ten human participants performed 40 min of fatiguing repetitive arm and neck exertions while SEMG data from the upper trapezius and sternocleidomastoid muscles were recorded. The ten of the most commonly used wavelet functions were used to conduct the DWT analysis. Spectral changes estimated using power of wavelet coefficients in the 12–23 Hz frequency band showed the highest sensitivity to fatigue induced by the dynamic repetitive exertions. Although most of the wavelet functions tested in this study reasonably demonstrated the expected power trend with fatigue development and recovery, the overall performance of the “Rbio3.1” wavelet in terms of power estimation and statistical significance was better than the remaining nine wavelets.

© 2013 Elsevier Ltd. All rights reserved.

### 1. Introduction

Work-related repetitive upper extremity exertions are a known cause of neck and shoulder musculoskeletal disorders (MSDs). In 2010, repetitive upper extremity exertions resulted in the highest number (median = 24) of days away from the work compared to all other types of exertions combined (median = 8) (BLS, 2011). The overuse of muscles, nerves, and/or joints caused by repetitive movements leads to muscle fatigue which is believed to be the precursor to most of the inflammatory-type neck and shoulder MSDs (Larsson et al., 2007). Therefore, accurate methods for muscle fatigue assessment are essential for the early detection and prevention of MSDs associated with repetitive upper extremity exertions.

A number of methods are used for the assessment of muscle fatigue generated by the work-related demands. Some of the most commonly used methods include evaluation of maximum voluntary contraction (Newham et al., 1991), endurance time (Garg et al., 2002), metabolite concentrations (Cady et al., 1989), perceived effort (Ahsberg et al., 2000), and subjective discomfort ratings (Öberg et al., 1994). Most of these methods are typically used in the evaluation of fatigue generated by heavy or sustained

static exertions (Vøllestad, 1997) and may not be receptive to the subtle fatigue-induced physiological changes caused by sub-maximal repetitive exertions. The muscle action potential characteristics are likely to change in response to the neuromuscular fatigue caused by sub-maximal exertions. The traditional methods used to evaluate changes in the action potential typically rely on metrics such as changes in the mean/median of the frequency spectrum obtained using fast Fourier transform (FFT) of muscle electromyography (Potvin, 1997). The FFT based estimation accurately quantifies the signal frequency content, i.e. how much of each frequency exists in the signal spectrum, but timing information, i.e. when a particular frequency component takes place in time, cannot be determined using the FFT method. For a stationary signal (all frequency components exist at all times), the timing information may be extraneous and shift in the power spectrum frequencies provides reliable indication of the muscle fatigue (Hostens et al., 2004). However, under repetitive dynamic conditions, the spectral changes of the non-stationary EMG signal estimated by FFT may not indicate the muscle fatigue accurately (Moshou et al., 2005). In such cases, the short time Fourier transform (STFT) is used, which implements window sizes of variable widths so that the stationary requirement is met. However, the window size approximation can constrain the signal spectrum estimation. For example, a short window size in STFT provides better time resolution, but

\* Corresponding author. Tel.: +1 (304) 293 9473; fax: +1 (304) 293 4970.

E-mail address: [Ashish.Nimbarte@mail.wvu.edu](mailto:Ashish.Nimbarte@mail.wvu.edu) (A.D. Nimbarte).

poor frequency resolution; while a relatively long window size provides better frequency resolution but poor time resolution (Hostens et al., 2004).

The discrete wavelet transform (DWT) provides a potential solution to this time and frequency resolution issue because of its ability to simultaneously elucidate local spectral and temporal information from a signal (Samar et al., 1999). It acts as a “mathematical microscope” in which one can observe different parts of the signal by adjusting the focus. Another advantage of DWT is the availability of various orthogonal wavelet functions that allow the most appropriate one to be chosen for the signal under investigation (Polikar, 2006). This is in contrast to the FFT analysis which is restricted to one feature morphology: the sinusoid. While sinusoid functions are useful in analyzing periodic and time-invariable phenomena, wavelets are well suited for the analysis of transient, time varying signals (Daubechies, 1990). A few previous studies have clearly stated that the wavelet transform is a more reliable method for the evaluation of fatigue induced spectral changes than Fourier transform, especially when the signal under investigation is non-stationary (Hua et al., 2007; Vukova et al., 2008).

Despite suitability of DWT for spectral analysis of non-stationary EMG signals, there is a lack of available data in the literature concerning its application for evaluation of muscle fatigue generated by work-related repetitive exertions. Therefore, the purpose of this study was to establish DWT analysis as a suitable method to conduct quantitative assessment of neck and shoulder muscle fatigue generated by repetitive exertions. The specific objectives of this study were to: (1) compare commonly used wavelet functions and identify the most appropriate one for analyzing neuromuscular fatigue of neck and shoulder muscles generated by repetitive exertions; (2) identify the frequency bands that show characteristic changes with the development of fatigue and recovery.

## 2. Methods

### 2.1. Protocol overview

In this study, ten of the most commonly used wavelet functions were used to analyze the SEMG data using discrete wavelet transform (DWT) analysis. The SEMG data were recorded during repetitive upper extremity exertions performed under normal and fatigued conditions. The neuromuscular fatigue was generated experimentally using repetitive upper extremity exertions performed over two 20 min sessions, with a 5 min break between the sessions. The activity of major neck and shoulder muscles responsible for these exertions i.e., right upper trapezius and left sternocleidomastoid muscles (contra-lateral to the direction of head rotation), were recorded using surface electromyography (SEMG). Seven levels of decomposition were used to compute power of the signal in different frequency bands. Power trends were statistically compared to identify wavelet functions and the frequency bands that are most sensitive to the fatigue induced spectral changes.

### 2.2. Participants

A convenient sample of ten healthy engineering graduate and undergraduate male students was used for data collection. The average age, weight, and height of the participants were 27(4.8) years, 71.12(9.30) kg, and 170.2(11.1) cm, respectively. The primary inclusion criteria used in this study required that the participants were free from any type of musculoskeletal disorders and had no history of neck and shoulder injury or notable neck pain. The Physical Activity Readiness Questionnaire (PAR-Q, Cana-

dian Society for Exercise Physiology) was used to screen participants for cardiac and other health problems (e.g., dizziness, chest pain, heart trouble). Participants who met the inclusion criteria were asked to read and sign a consent form approved by the local Institutional Review Board.

### 2.3. Apparatus/tools

#### 2.3.1. Electromyography (EMG) system

A 16-channel telemetry EMG system consisting of a Telemetry 2400T wireless transmitter, pre-amplified lead wires, and disposable, self-adhesive Ag/AgCl snap electrodes was used to collect SEMG data. The bipolar Ag/AgCl pre-gelled surface electrodes (1 cm diameter, inter-electrode distance is 2 cm) connect to the Telemetry 2400T transmitter via pre-amplified lead wires. The pre-amplifier on the lead wires have CMRR > 100 dB, Input Impedance > 100 M $\Omega$ , and base gain of 500. The range of the band pass filter was 10–500 Hz (Noraxon, 2011). The frequency of EMG data acquisition was set at 1500 Hz.

#### 2.3.2. Workstation

A custom-built workstation was used to simulate repetitive upper extremity exertions. This workstation consists of two adjustable orthogonally-placed work surfaces (Fig. 1b). If a participant is facing surface 1, then surface 2 is to the right of the participant. Thirty small cylindrical containers (diameter = 3.0 cm; height = 5.0 cm; weight = 50 g) were used to perform the repetitive upper extremity exertions. A stand containing these cylinders was placed on surface 1, which was adjusted to the participant's fingertip height. The height of surface 2 was adjusted to the standing eye height of the participant.

### 2.4. Experimental protocol

Upon arriving at the laboratory, each participant was introduced to the equipment, data collection procedures, and specifics of the experimental tasks. The demographics and anthropometric measures of the participant were recorded and they were then subsequently prepared for SEMG data collection. SEMG from the left sternocleidomastoid muscle was recorded by placing an electrode along a line drawn from the sternal notch to the mastoid process, at 1/3 the distance from the mastoid process (Nimbarte et al., 2010, 2012). SEMG from the right upper trapezius muscle was recorded by placing an electrode along a line joining the acromion and C7, at 1/3 the distance from the acromion process (Nimbarte et al., 2010, 2012). The skin underneath the anatomical landmarks was shaved (if needed), and cleaned with 70% alcohol, prior to the placement of the SEMG electrodes.

Next, the participant performed repetitive upper extremity exertions to manually transfer 30 cylindrical containers from surface 1 to surface 2. Once all 30 containers have been moved from surface 1 to surface 2 (stocking operation), the participant began the un-stocking operation, i.e. transferring the containers back to surface 1 from surface 2. These exertions closely replicate the top shelf stocking and unstocking operations performed by a super market grocery clerk (Fig. 1a). Each motion involved 90° of flexion and abduction of the upper arm, 60–90° of head-neck rotation and 10–20° of head-neck extension. Stocking and unstocking operations were performed continuously for a duration of 20 min (session 1). A rest period of 5 min was provided at the end of session 1. After the rest period, the participant continued the same stocking and unstocking operation for another 20 min (session 2).

SEMG data was recorded continuously during sessions 1 and 2. In addition, at the end of each session, the participant was asked to report discomfort in the right shoulder region and the left anterior neck region using Borg's subjective rating scale (Borg, 1998). The

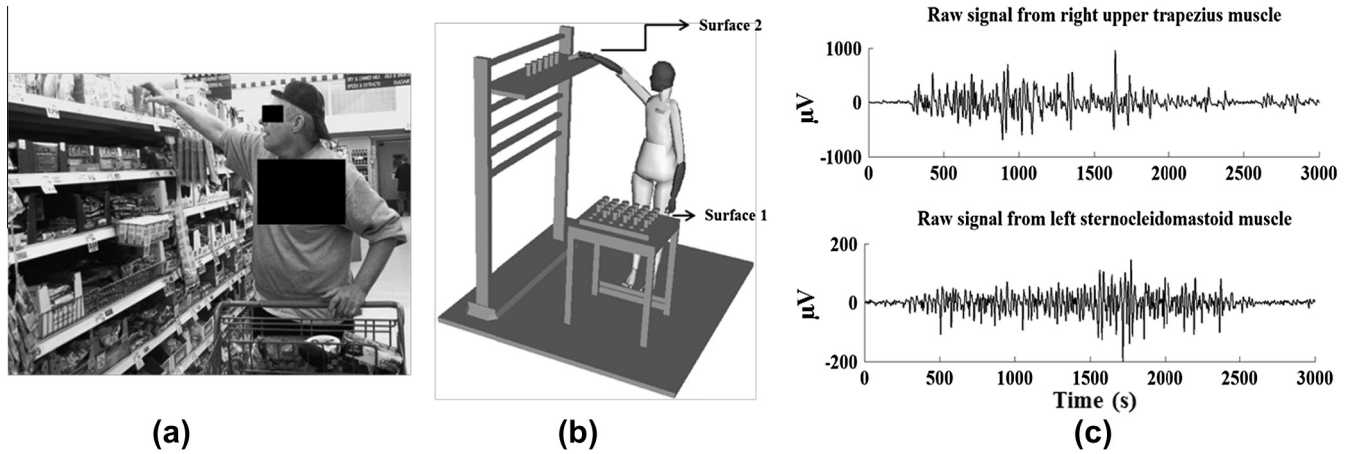


**Fig. 1.** (a) A picture from a grocery store showing the height of the top shelves, (b) custom-built workstation, and (c) Raw EMG signal during a stocking repetition.

duration of individual stocking and unstocking operations were also recorded during sessions 1 and 2.

### 2.5. Data processing

SEMG signal during the first five and last five stocking motions in sessions 1 and 2 were selected for the DWT analysis. The time windows corresponding to these exertions were obtained based on the visual inspection of EMG activation. From the onset of the EMG signal, a time window of 2 s was used for selecting the EMG signal for further analysis. This selection was based on cycle time analysis. The individual user used an average duration of 2 s to complete the stocking or unstocking operation.

At each DWT decomposition, SEMG signal  $X$  (Fig. 1c) was processed through a series of high-pass and low-pass filters to analyze the high and low frequencies. The down-sampled output of the high-pass and low-pass filters are the detail coefficients (CD) and approximate coefficients (CA), respectively (Fig. 2a) (Polikar, 2006).

The procedure was repeated for subsequent decompositions of the SEMG signal into seven levels. Frequency bandwidth (B) at different decomposition levels (L) is obtained using the following equation (Cong et al., 2012) and is diagrammatically represented in Fig. 2.

$$B = f_s / 2^{(L+1)} \quad (1)$$

Here  $f_s$  represents sampling frequency.

The wavelet toolbox from Matlab (R2011a) was used to conduct the DWT analysis. The decomposed signal was reconstructed through synthesis filters (Hong-tu and Jing, 2010). The reconstructed signal ( $X'$ ) could be expressed using the following vector:

$$X' = (A_7, D_7, D_6, D_5, D_4, D_3, D_2, D_1) \quad (2)$$

where  $A_7$  represents approximation coefficients at the 7th reconstruction level and  $D_1$ – $D_7$  represents detail coefficients at the 1st to 7th reconstruction levels, respectively (Fig. 2b).

According to the characteristics of the orthogonal wavelet transform, the total power of the time window  $P$  is equal to the sum of the components  $P_j$ . Hence,  $P = P_{j0} + \sum_{j=1}^7 P_j$ , where  $P_j$  is the power spectrum of each detail level  $j$  and  $P_{j0}$  is the power spectrum of the approximate level. The probability of the signal power at decomposition scale  $j$ , is  $w_j = P_j / P$  and the total probability is  $\sum_j w_j = 1$  (Hu et al., 2008).

The higher amplitude values reflect the time localization of the corresponding frequency sub-band on the time–frequency region. Taking the high-frequency reconstruction scale as an independent signal (Fig. 2c), the energy, or the amount of power at the  $j$ th level,

could be computed by integrating the squares of wavelet coefficient values in discrete time sequence of 2 s.

$$P_j = \sum_{k=1}^{3000} |C_j(k)|^2 \quad (3)$$

where  $C(1)$ – $C(3000)$  are the detail coefficient values at  $j$ th reconstruction level.

The ability of DWT to estimate features from the SEMG signal is dependent upon the impulse response of the high pass and low pass filters which is a function of the wavelet function used for signal decomposition. Although there is no well-defined rule for selecting a specific wavelet function for a particular analysis, the properties of time and frequency localization make one wavelet function more suitable for a given application than another. Thus, the power of the different frequency bands computed using these 10 wavelet functions (Table 1) contributed in choosing the best one that could extract the required frequency components from a SEMG signal.

The mean power of a frequency sub-band at four different time instances was computed by averaging the power of the SEMG signal during five stocking repetitions. For example, five stocking repetitions performed at the beginning of session 1 were used to estimate mean power at time instance  $T_0$ .

### 2.6. Statistical analysis

The equality of variance and normality test demonstrated that the assumption of the homoscedasticity and normal distribution was true. Therefore, fatigue induced changes in the power of different frequency bands were analyzed using a mixed model analysis of variance (ANOVA). The fixed effect of time was set at four levels: exertions at the beginning and the end of session 1 ( $T_0$  and  $T_{20}$ ) and session 2 ( $T_{25}$  and  $T_{45}$ ). 'Participant' was treated as a random factor. The hypothesis was tested for the effect of time at 95% confidence level in SAS version 9.2. Significant effects were further evaluated by using Tukey's all-pairwise comparison test. A scoring system based on the  $P$ -values of Tukey's multiple comparison tests was used to assess the performance of different wavelets in distinguishing power levels at different time instances. A score of '1' was assigned to a comparison with  $P \leq 0.05$ . For  $P > 0.05$  a score of '0' was assigned.

## 3. Results

The participants completed mean 19.5(0.71) and 19.8(0.79) stocking operations during sessions 1 and 2, respectively. Mean duration of one stocking operation was 61.61(±2.32) and 60.69(±2.39) seconds during sessions 1 and 2, respectively.

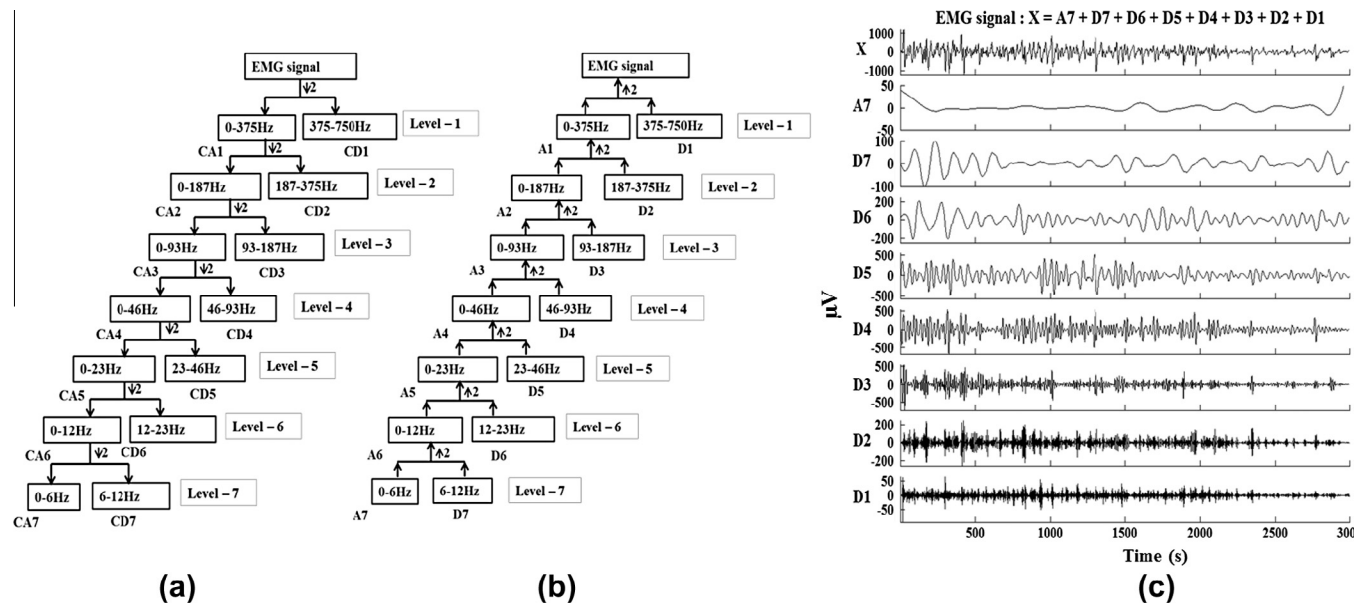


**Fig. 2.** Seven level of: (a) decomposition and (b) reconstruction algorithm of DWT used in this study (c) SEMG signal from right upper trapezius muscle and its seven level of decomposition using Db5 wavelet.

**Table 1**  
Selected wavelet functions in this study.

Number	Wavelet function	Wavelet family	Studies used
1	Bior1.5	Biorthogonal	Khezri and Jahed (2008) recommended bior1.5 as the best denoising estimation of SEMG signals
2	Bior3.1	Biorthogonal	
3	Rbio3.1	Reverse Biorthogonal	Bousbia-Salah et al. (2011) recommended bior3.1 as the best among biorthogonal family for bio-signal compression
4	Coif5	Coiflet	Rbio3.1 was used in few studies along with other wavelet functions to extract muscle activity features and denoise the SEMG signals (Phinyomark et al., 2009a,b)
5	Db2	Daubechies	Coif5 provided the best reconstruction of SEMG signal in a study performed by Phinyomark and Phukpattaranont (2009)
6	Db5		Hussein et al., (2009) found db2 as the best choice among other wavelets to denoise SEMG signals
7	Db45		Ren et al. (2006) used wavelet function db5 to denoise SEMG signals in their research
8	Haar	Haar	Reaz et al. (2006) found that db45 wavelet function most significantly presented the change in the power spectrum properties of resting and maximum contraction stage of walking exertions
9	Sym4	Symlet	Haar was used by Lauer et al., (2003) for SEMG decomposition to quantify onset and offset of muscle activity in a human gait study
10	Sym5		Kumar et al. (2003) found significant differences between the power of fatigued and non-fatigued SEMG signal using sym4 and sym5 wavelet functions

A mean discomfort of 5 (=slight moderate discomfort) and 4 (=slight discomfort) in the right posterior shoulder and left anterior neck regions, respectively, were reported by the participants at the end of session 1 ( $T_{20}$ ). At the end of session 2 ( $T_{45}$ ), for these re-

gions, mean discomforts of 7 (=some discomfort) and 5, were reported (Fig. 3).

Mean power of the SEMG signal in different frequency bands computed using Coif5 wavelet is shown in Fig. 4. In general, a very low power was observed in the 375–750 Hz, 187–375 Hz, and 6–12 Hz bands and therefore these bands were ignored for further statistical analysis. The highest power was observed in the frequency bands of 46–93 Hz, followed by the frequency bands of 93–187 Hz, 23–46 Hz, and 12–23 Hz. This trend of power with respect to different frequency bands was consistent between all the wavelet functions.

The effect of time on the power in the 46–93 Hz and 93–187 Hz frequency bands was statistically not significant for any of the 10 wavelets (Table 2). For the upper trapezius muscle, the effect of time on the power in the 12–23 Hz and 23–46 Hz frequency bands was statistically significant for most of the wavelets (Table 2). For the sternocleidomastoid muscle, the effect of time on the power was statistically significant for most of the wavelets for the 12–23 Hz frequency band. However, power in the 23–46 Hz frequency

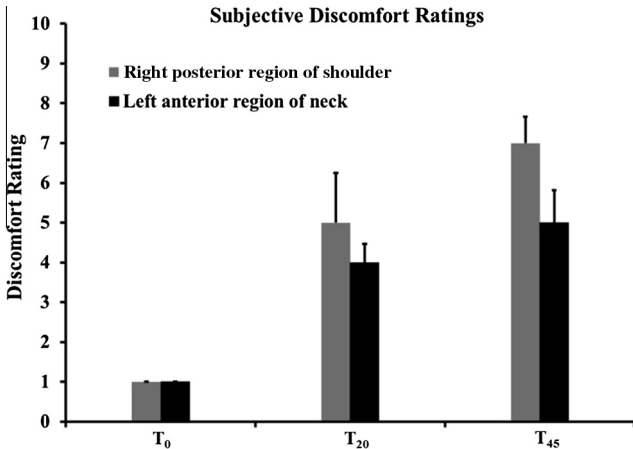


**Fig. 3.** Subjective discomfort scores at different time instances.  $T_0$ ,  $T_{20}$ , and  $T_{45}$  refer to 1st minute, 20th minute, and 45th minute of the exertions, respectively.



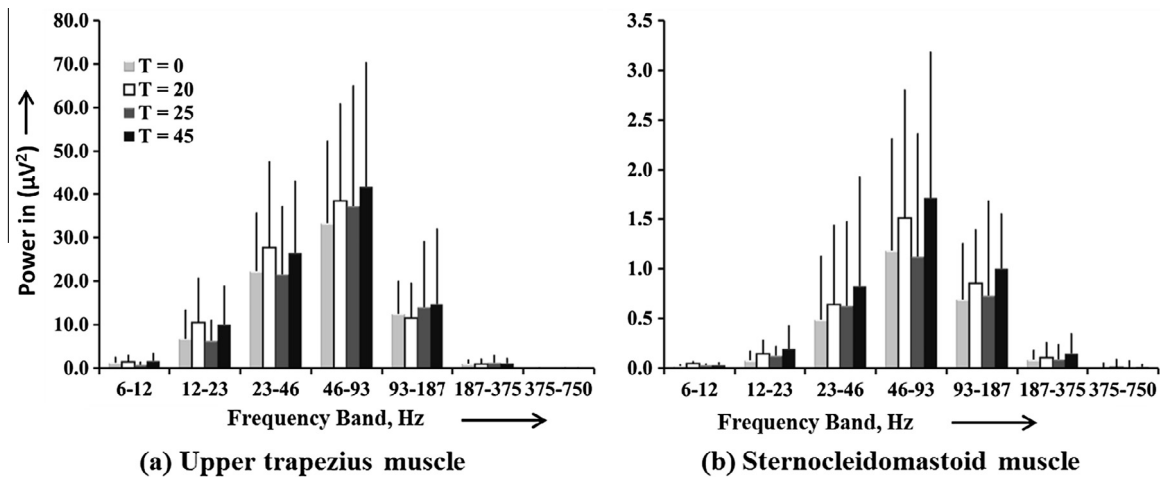


**Fig. 4.** Mean power ( $\mu V^2$ ) in different frequency bands as a function of time for Coif5 wavelet function for (a) right trapezius muscle (b) left sternocleidomastoid muscle.  $T_0$ ,  $T_{20}$ ,  $T_{25}$ , and  $T_{45}$  refer to 1st minute, 20th minute, 25th and 45th minute of the exertions, respectively.

band was found to be statistically significant only for the Rbio3.1 wavelet (Table 2).

Tukey's all-pairwise multiple comparison test showed a distinct pattern of statistical significance between the time instances for different wavelets (Table 3). For the upper trapezius muscle, statistical significance was observed for the increase in power from  $T_0$  to  $T_{20}$ ,  $T_{20}$  to  $T_{45}$ , and  $T_0$  to  $T_{45}$  for most of the wavelets. Statistical significance was also observed for the decline in power from  $T_{20}$  to  $T_{25}$  for most of the wavelets. However, the most consistent statistical trend for the increase in power with the development of fatigue and decline in power with rest, signified by the highest overall score (Table 3 and Fig. 5), was observed for the Rbio3.1 wavelet. Similarly, the 12–23 Hz frequency band showed a more consistent statistical trend for the power with fatigue development and rest.

For the sternocleidomastoid muscle, statistical significance for the increase in power in the 12–23 Hz frequency band was observed from  $T_0$  to  $T_{45}$  for all wavelets. A few wavelets also showed a statistically significant increase in power in the 12–23 Hz frequency band from  $T_0$  to  $T_{20}$  and from  $T_{20}$  to  $T_{45}$ . None of the wavelets showed statistical significance for the decline in power from  $T_{20}$  to  $T_{25}$ . Compared to the 12–23 Hz frequency band, statistical significance for the power trend in the 23–46 Hz frequency band was observed only for the Rbio3.1 wavelet. Similar to the upper trapezius muscle, the Rbio3.1 wavelet and 12–23 Hz frequency band showed the most consistent statistical trend for the power with fatigue development and rest for the sternocleidomastoid muscle (Table 3 and Fig. 5).

Time–frequency representation of DWT for the Rbio3.1 wavelet was plotted using a scalogram (Fig. 6) to show the energy density of different levels. SEMG signals at four different time occasions

were combined together to portray a complete SEMG signal in a particular task. At the 5th, 6th, and 7th levels, a larger number of darker bands occurring at  $T_{20}$  and  $T_{45}$  compared to  $T_0$  and  $T_{25}$  indicated a higher amount of energy for the lower frequency bands towards the end of the sessions 1 and 2. A substantial increase in the number of darker bands was observed at  $T_{45}$  compared to  $T_{25}$  further indicating a higher increase in the amount of the energy for exertions performed at the end of session 2 than session 1.

#### 4. Discussion

Fatigue induced spectral changes in the SEMG signal by repetitive exertions were assessed using DWT analysis. Ten of the most commonly used wavelet functions were used to perform the DWT analysis. Continuously performed repetitive exertions significantly increased the subjective discomfort in the regions of the neck and shoulder corresponding to the locations of the right upper trapezius and left sternocleidomastoid muscles, confirming the development of fatigue in these muscles. The power of the lower frequency wavelet coefficients showed consistent and statistically significant trends with the development of fatigue. Selection of the wavelet function used to perform DWT analysis also seems to affect the assessment of spectral changes in the SEMG signal induced by fatiguing repetitive exertions.

Wavelet coefficients and the resulting power in the 12–23 Hz frequency band provided the most accurate manifestation of fatigue induced by repetitive exertions. In this frequency band, a significant increase in the power with the development of fatigue was observed for most of the wavelet functions. Additionally, a drop in the power level following the rest period was also observed

**Table 2**

P-values for the effect of time on the power in different frequency bands estimated by various wavelet functions for the upper trapezius and the sternocleidomastoid muscles. Statistically significant values are marked with asterisks (\*).

	Bior1.5	Bior3.1	Rbio3.1	Coif5	Db2	Db5	Db45	Haar	Sym4	Sym5
Frequency Band (Hz)	<i>Upper trapezius muscle</i>									
12–23	0.03*	0.02*	0.03*	0.02*	0.03*	0.03*	0.04*	0.04*	0.03*	0.02*
23–46	0.04*	0.42	0.03*	0.13	0.04*	0.04*	0.13	0.19	0.2	0.04*
46–93	0.54	0.52	0.12	0.44	0.66	0.59	0.37	0.22	0.28	0.63
93–187	0.64	0.61	0.29	0.69	0.67	0.68	0.72	0.65	0.67	0.68
	<i>Sternocleidomastoid muscle</i>									
12–23	0.15	0.03*	0.03*	0.04*	0.04*	0.17	0.3	0.18	0.04*	0.2
23–46	0.42	0.37	0.03*	0.57	0.31	0.45	0.38	0.48	0.44	0.37
46–93	0.69	0.76	0.65	0.5	0.66	0.55	0.62	0.59	0.51	0.55
93–187	0.6	0.51	0.59	0.66	0.59	0.63	0.57	0.56	0.63	0.69

**Table 3**

P-values of Tukey's multiple comparison tests for the effect of time on the power in different frequency bands estimated by various wavelets for upper trapezius and sternocleidomastoid muscles.  $T_0$ ,  $T_{20}$ , and  $T_{45}$  refer to 1st minute, 20th minute, and 45th minute of the exertions, respectively.

	Time instances	Bior1.5	Bior3.1	Rbio3.1	Coif5	Db2	Db5	Db45	Haar	Sym4	Sym5
<b>Upper trapezius muscle</b>											
Frequency Band (Hz) 12–23	$T_0$ vs $T_{20}$	0.04*	0.02*	0.01*	0.03*	0.02*	0.04*	0.06	0.07	0.03*	0.03*
	$T_0$ vs $T_{25}$	0.81	0.39	0.79	0.76	0.60	0.55	0.41	0.97	0.57	0.42
	$T_0$ vs $T_{45}$	0.04*	0.01*	0.02*	0.04*	0.16	0.08	0.18	0.03*	0.12	0.16
	$T_{20}$ vs $T_{25}$	0.02*	0.04*	0.03*	0.01*	0.01*	0.01*	0.01*	0.07	0.01*	0.01*
	$T_{20}$ vs $T_{45}$	0.99	0.40	0.70	0.76	0.36	0.72	0.55	0.75	0.48	0.43
	$T_{25}$ vs $T_{45}$	0.03*	0.02*	0.02*	0.03*	0.06	0.02*	0.04*	0.04*	0.04*	0.03*
23–46	$T_0$ vs $T_{20}$	0.06	0.18	0.04*	0.08*	0.04*	0.04*	0.08	0.14	0.12	0.04*
	$T_0$ vs $T_{25}$	0.65	0.49	0.17	0.82	0.98	0.95	0.77	0.58	0.85	0.93
	$T_0$ vs $T_{45}$	0.13	0.14	0.04*	0.17	0.03*	0.04*	0.18	0.40	0.20	0.04*
	$T_{20}$ vs $T_{25}$	0.02*	0.50	0.01*	0.05*	0.04*	0.04*	0.04*	0.04*	0.08	0.04*
	$T_{20}$ vs $T_{45}$	0.63	0.90	0.52	0.69	0.89	0.92	0.68	0.50	0.77	0.99
	$T_{25}$ vs $T_{45}$	0.05*	0.43	0.02*	0.11	0.03*	0.03*	0.11	0.17	0.14	0.04*
Overall score		6	4	<b>8</b>	6	6	7	3	3	3	7
Rank		3	4	<b>1</b>	3	3	2	5	5	5	2
<b>Sternocleidomastoid muscle</b>											
Frequency Band (Hz) 12–23	$T_0$ vs $T_{20}$	0.21	0.04*	0.04*	0.18	0.36	0.27	0.22	0.11	0.15	0.31
	$T_0$ vs $T_{25}$	0.43	0.71	0.49	0.42	0.63	0.42	0.36	0.32	0.68	0.46
	$T_0$ vs $T_{45}$	0.03*	0.01*	0.02*	0.01*	0.03*	0.03*	0.07	0.04*	0.04*	0.04*
	$T_{20}$ vs $T_{25}$	0.64	0.35	0.40	0.58	0.66	0.77	0.76	0.51	0.45	0.77
	$T_{20}$ vs $T_{45}$	0.29	0.18	0.36	0.20	0.17	0.25	0.51	0.62	0.35	0.26
	$T_{25}$ vs $T_{45}$	0.13	0.03*	0.04*	0.04*	0.05*	0.15	0.33	0.25	0.04*	0.16
23–46	$T_0$ vs $T_{20}$	0.29	0.27	0.36	0.52	0.35	0.50	0.28	0.26	0.43	0.46
	$T_0$ vs $T_{25}$	0.67	0.56	0.61	0.56	0.80	0.73	0.64	0.50	0.52	0.77
	$T_0$ vs $T_{45}$	0.13	0.10	0.03*	0.17	0.09	0.13	0.11	0.14	0.11	0.10
	$T_{20}$ vs $T_{25}$	0.52	0.59	0.69	0.95	0.49	0.74	0.53	0.64	0.88	0.66
	$T_{20}$ vs $T_{45}$	0.62	0.55	0.20	0.45	0.42	0.38	0.58	0.72	0.40	0.35
	$T_{25}$ vs $T_{45}$	0.26	0.26	0.02*	0.41	0.14	0.23	0.24	0.41	0.33	0.17
Overall score		1	3	<b>5</b>	2	2	1	0	1	2	1
Rank		4	2	<b>1</b>	3	3	4	5	4	3	4

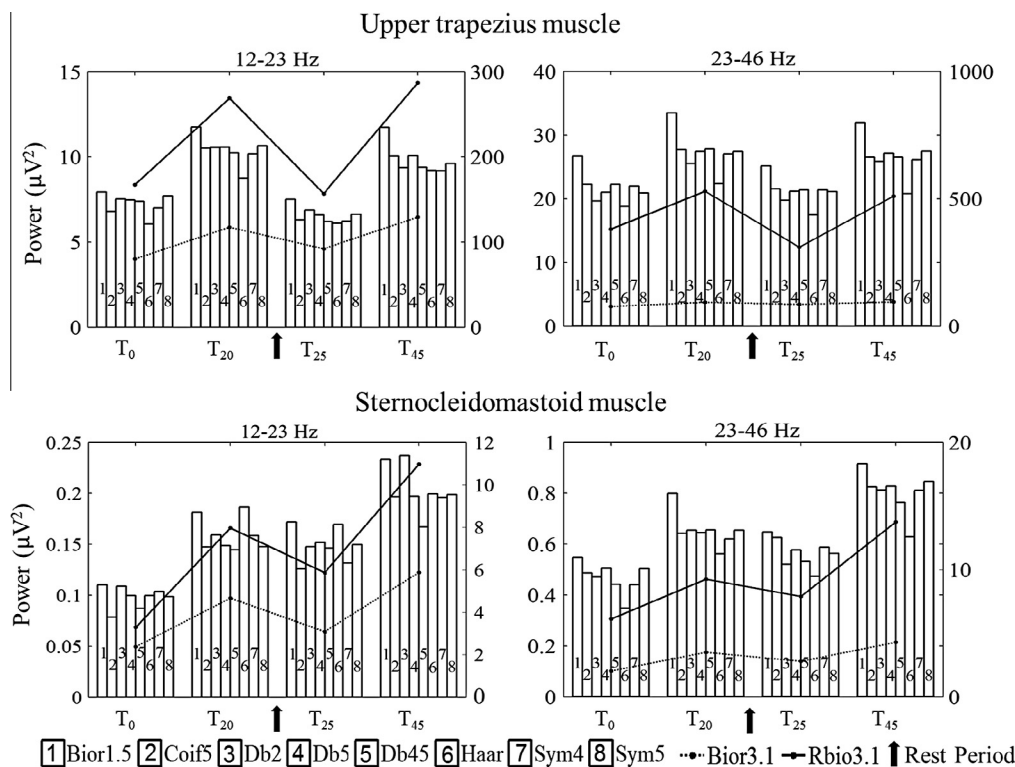


**Fig. 5.** Mean power in 12–23 Hz and 23–46 Hz frequency bands at different time instances for right upper trapezius and left sternocleidomastoid muscles.  $T_0$ ,  $T_{20}$ ,  $T_{25}$ , and  $T_{45}$  refer to 1st minute, 20th minute, 25th and 45th minute of the exertions, respectively. Power estimated using Rbio3.1 and Bior3.1 wavelets was plotted using a secondary axis.

consistently in this frequency band. The characteristic changes in the power of the lower frequency band with the onset and devel-

opment of fatigue observed in this study is consistent with previous studies. Kumar et al. (2003) found a significant increase in

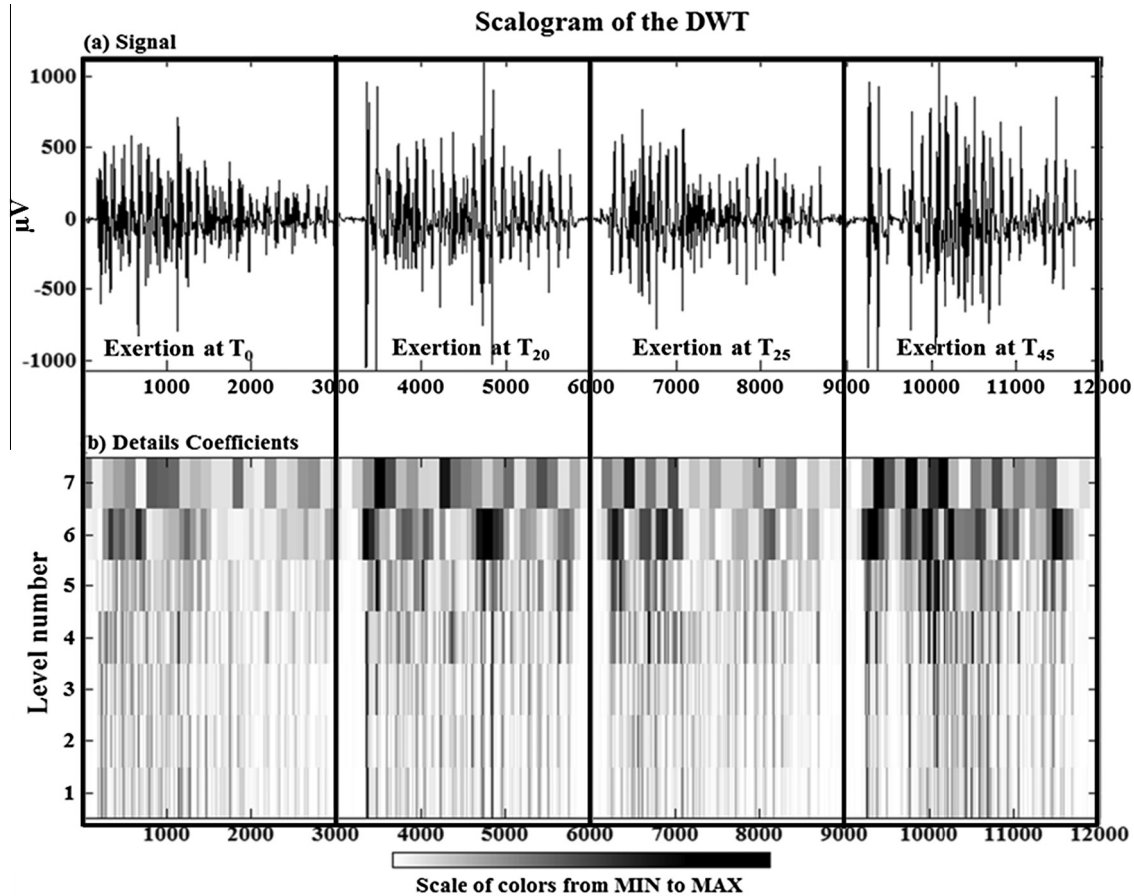


**Fig. 6.** Illustration of the raw SEMG signal and corresponding intensity pattern computed using DWT with Rbio3.1.  $T_0$ ,  $T_{20}$ ,  $T_{25}$ , and  $T_{45}$  refer to 1st minute, 20th minute, 25th and 45th minute of the exertions, respectively.

the power of the 6–24 Hz frequency band when SEMG signals from the fatigued and non-fatigued bicep-brachii muscle were compared against each other. Dolan et al. (1995) also reported that fatigue-induced changes increased the power in the 5–30 Hz frequency band for the erector spinae muscle. In this study, lead wires used to collect SEMG data had a band-pass filter of 10–500 Hz, and therefore, very low power in the 6–12 Hz frequency band was observed. Augmentation of motor units' firing rate is reasoned for the increase in the low frequency content of the SEMG signal. Under fatigued condition, changes in the concentrations of calcium ions ( $\text{Ca}^{2+}$ ) and lactic acid negatively impact muscle fiber excitation–contraction coupling (Allen, 2004; Kurebayashi and Ogawa, 2001). This elevates the motor unit firing rate in order to maintain similar force exertion levels (Vukova et al., 2008).

Contrary to a few previous studies (Sparto et al., 2000; Vukova et al., 2008), power of the high frequency wavelet coefficients showed an inconsistent trend with the development of fatigue in this study. High frequency signals reflect changes in the conduction velocity, which has been shown to decline with the development of fatigue, reducing the high frequency content. However, noticeable change in the conduction velocity was generally observed during moderate to heavy force exertion levels (usually >15–20% MVC) (Krogh-Lund and Jørgensen, 1992). Since the force exertion levels used in this study were very small ( $\sim$ 2–5% MVC for most of the participants), changes in the conduction velocity may not have been sufficient to exhibit consistent alteration (decline) in the power of high frequency wavelet coefficients.

Spectral changes estimated by DWT analysis were found to be dependent on the wavelet function used in the analysis. Shape matching of a wavelet function with the trains of motor unit action

potential affects the detail coefficients estimated by DWT analysis. High amplitudes of detail coefficients signify a good matching, whereas mismatch produces low amplitudes (Samar et al., 1999). Although most of the wavelet functions tested in this study reasonably demonstrate expected power trend with fatigue development and recovery, some wavelets performed better than others. Previously, Kumar et al. (2003), compared performance of seven wavelets to estimate fatigue generated in the biceps-brachii muscle using DWT. The 'Sym4' and 'Sym5' wavelets were found to estimate fatigue induced spectral changes more accurately than the 'haar', 'Db2', 'Db3', 'Db4', and 'Db5' wavelets. Although 'Sym4' and 'Sym5' showed a characteristic power trend for the upper trapezius muscle in the 12–23 Hz frequency band, a more consistent and statistically significant trend was observed for the Bior1.5, Bior3.1, Rbio3.1, and Coif5 wavelet functions for the upper trapezius and sternocleidomastoid muscles in the 12–23 Hz and 23–46 Hz frequency bands. Power estimated by the Bior3.1 and Rbio3.1 wavelets were much higher than the Bior1.5 and Coif5 wavelets. In addition, the Rbio3.1 wavelet also showed a statistically consistent and meaningful trend not only in the 12–23 Hz bands, but also in the 23–43 Hz frequency bands. Overall, the results of this study indicate that the "Reverse Biorthogonal with 3.1 scales (Rbio3.1)" wavelet function most accurately predicted the fatigue induced spectral changes caused by repetitive exertions with high sensitivity out of the ten wavelets tested in this study.

The stocking task used in this study was designed to generate fatigue in the neck and shoulder muscles through sustained repetitive exertions. However, for the sternocleidomastoid muscle, the power of the detail coefficients was much lower than the upper trapezius muscle. Moreover, statistical significance was observed

at fewer instances for the sternocleidomastoid muscle than for the upper trapezius muscle. It is likely that participants may have compensated for their head motion using eye movements during these tasks, resulting in lower levels of exertion by the sternocleidomastoid muscle. Future studies should evaluate physical motion in addition to the SEMG spectral pattern in order to enhance our understanding of objective assessment of fatigue generated by work-related repetitive exertions. Future studies should also compare the effects of gender and different force exertion conditions.

## 5. Conclusions

DWT based multi-resolution analysis of biological signals has gained popularity in the recent years. For repetitive sub-maximal exertions by the upper extremity and neck muscles, which are the hallmark of work at various industries, it is highly likely that the SEMG signal is not stationary. This study provides quantitative data that demonstrates spectral changes estimated by DWT sensitively predict the fatigue in the major neck and shoulder muscles generated by sub-maximal dynamic repetitive exertions. The spectral change in the lower frequency band of 12–23 Hz was found to be the most sensitive to the fatigue generated by the sub-maximal dynamic repetitive exertions. Among the 10 most popular wavelets that have been used previously to analyze SEMG data, the overall performance of the Rbio3.1 wavelet was the best in the assessment of fatigue generated by the sub-maximal dynamic repetitive exertions.

## References

- Ahsberg E, Gamberale F, Gustafsson K. Perceived fatigue after mental work: an experimental evaluation of a fatigue inventory. *Ergonomics* 2000;43:252–68.
- Allen D. Skeletal muscle function: role of ionic changes in fatigue, damage and disease. *Clin Exp Pharmacol Physiol* 2004;31:485–93.
- BLS. Nonfatal occupational injuries and illnesses requiring days away from work, 2010; 2011.
- Borg G. Borg's perceived exertion and pain scales. Human Kinetics Publishers; 1998.
- Cady E, Jones D, Lynn J, Newham D. Changes in force and intracellular metabolites during fatigue of human skeletal muscle. *J Physiol* 1989;418:311.
- Bousbia-Salah A, Ait-Ameur M, Talha-Kedir M. Biorthogonal wavelet for EEG signal compression. *ACM*; 2011. p. 9.
- Cong F, Huang Y, Kalyakin I, Li H, Huttunen-Scott T, Lyytinen H, et al. Frequency-response-based wavelet decomposition for extracting children's mismatch negativity elicited by uninterrupted sound. *J Med Biol Eng* 2012;32:205–13.
- Daubechies I. The wavelet transform, time-frequency localization and signal analysis. *Inform Theor IEEE Trans* 1990;36:961–1005.
- Dolan P, Mannion A, Adams M. Fatigue of the erector spinae muscles: a quantitative assessment using "frequency banding" of the surface electromyography signal. *Spine* 1995;20:149.
- Garg A, Hegmann KT, Schwoerer BJ, Kapellusch JM. The effect of maximum voluntary contraction on endurance times for the shoulder girdle. *Int J Ind Ergon* 2002;30:103–13.
- Hong-tu Z, Jing Y. The Wavelet Decomposition and Reconstruction based on the Matlab. In: Proceedings of the Third International Symposium on Electronic Commerce and Security Workshops (ISECS '10), Guangzhou, PR China, 29–31, July; 2010. p. 143–45.
- Hostens I, Seghers J, Spaepen A, Ramon H. Validation of the wavelet spectral estimation technique in biceps brachii and brachioradialis fatigue assessment during prolonged low-level static and dynamic contractions. *J Electromyogr Kinesiol* 2004;14:205–15.
- Hu GS, Zhu FF, Ren Z. Power quality disturbance identification using wavelet packet energy entropy and weighted support vector machines. *Expert Syst Appl* 2008;35:143–9.
- Hua C, El Hajj Dib I, Antoni J, Marque C. Analysis of muscular fatigue during cyclic dynamic movement. *engineering in medicine and biology society*, 2007 EMBS 2007. In: 29th Annual international conference of the IEEE; 2007. p. 1880–3.
- Hussain M, Reaz M, Mohd-Yasin F, Ibrahim M. Electromyography signal analysis using wavelet transform and higher order statistics to determine muscle contraction. *Expert Systems*. 2009;26:35–48.
- Khezri M, Jahed M. Surface Electromyogram signal estimation based on wavelet thresholding technique. *Engineering in Medicine and Biology Society*, 2008 EMBS 2008 30th Annual International Conference of the IEEE 2008. p. 4752–5.
- Krogh-Lund C, Jørgensen K. Modification of myo-electric power spectrum in fatigue from 15% maximal voluntary contraction of human elbow flexor muscles, to limit of endurance: reflection of conduction velocity variation and/or centrally mediated mechanisms? *Eur J Appl Physiol* 1992;64:359–70.
- Kumar DK, Pah ND, Bradley A. Wavelet analysis of surface electromyography. *Neural Syst Rehab Eng*, IEEE Trans 2003;11:400–6.
- Kurebayashi N, Ogawa Y. Depletion of Ca<sup>2+</sup> in the sarcoplasmic reticulum stimulates Ca<sup>2+</sup> entry into mouse skeletal muscle fibres. *J Physiol* 2001;533:185–99.
- Lauer R, Loughton C, Orlin M, Smith B. Wavelet decomposition for the identification of EMG activity in the gait cycle. *IEEE*; 2003. p. 142–3.
- Larsson B, Sogaard K, Rosendal L. Work related neck-shoulder pain: a review on magnitude, risk factors, biochemical characteristics, clinical picture and preventive interventions. *Best Practice Res Clin Rheumatol* 2007;21:447–63.
- Moshou D, Hostens I, Papaioannou G, Ramon H. Dynamic muscle fatigue detection using self-organizing maps. *Appl Soft Comput* 2005;5:391–8.
- Newham D, McCarthy T, Turner J. Voluntary activation of human quadriceps during and after isokinetic exercise. *J Appl Physiol* 1991;71:2122.
- Nimbarte AD, Aghazadeh F, Ikuma LH, HARVEY CM. Neck disorders among construction workers: Understanding the physical loads on the cervical spine during static lifting tasks. *Ind Health* 2010;48:145–53.
- Nimbarte AD, Al Hassan MJ, Guffey SE, Myers WR. Influence of psychosocial stress and personality type on the biomechanical loading of neck and shoulder muscles. *Int J Ind Ergon* 2012;42:397–405.
- Noraxon. Arizona. USA; 2011. <[http://www.noraxon.com/products/instruments/telemetry\\_system.php3](http://www.noraxon.com/products/instruments/telemetry_system.php3)>.
- Öberg T, Sandsjö L, Kadefors R. Subjective and objective evaluation of shoulder muscle fatigue. *Ergonomics* 1994;37:1323–33.
- Phinyomark A, Limsakul C, Phukpattaranont P. A comparative study of wavelet denoising for multifunction myoelectric control. *IEEE*; 2009a. p. 21–5.
- Phinyomark A, Limsakul C, Phukpattaranont P. An optimal wavelet function based on wavelet denoising for multifunction myoelectric control. *IEEE*; 2009b. p. 1098–101.
- Phinyomark A, Phukpattaranont CLP. Evaluation of wavelet function based on robust emg feature extraction. 2009. p. 277281.
- Polikar R. The wavelet tutorial. Internet Resources; 2006. <<http://engineeringrowan.edu/polikar/WAVELETS/WTtutorial.html>>.
- Potvin J. Effects of muscle kinematics on surface EMG amplitude and frequency during fatiguing dynamic contractions. *J Appl Physiol* 1997;82:144.
- Reaz M, Hussain M, Mohd-Yasin F. EMG analysis using wavelet functions to determine muscle contraction. *IEEE*; 2006. p. 132–44.
- Ren X, Hu X, Wang Z, Yan Z. MUAP extraction and classification based on wavelet transform and ICA for EMG decomposition. *Medical and Biological Engineering and Computing*. 2006;44:371–82.
- Samar VJ, Bopardikar A, Rao R, Swartz K. Wavelet analysis of neuroelectric waveforms: a conceptual tutorial. *Brain Lang* 1999;66:7–60.
- Sparto PJ, Parnianpour M, Barria EA, Jagadeesh JM. Wavelet and short-time Fourier transform analysis of electromyography for detection of back muscle fatigue. *Rehab Eng IEEE Trans* 2000;8:433–6.
- Vøllestad NK. Measurement of human muscle fatigue. *J Neurosci Methods* 1997;74:219–27.
- Vukova T, Vydevska-Chichova M, Radicheva N. Fatigue-induced changes in muscle fiber action potentials estimated by wavelet analysis. *J Electromyogr Kinesiol* 2008;18:397–409.



**Suman Kanti Chowdhury** is a PhD student at the faculty of Industrial and Management System Engineering of West Virginia University. He received his M.S. degree in Industrial Engineering from West Virginia University in 2012, and received his B.E. degree in Industrial and Production Engineering from Bangladesh University of Engineering and Technology, Bangladesh in 2006. His research interest is in the areas of Industrial Ergonomics and Human Factors Engineering. His recent research focuses on estimation of neck and shoulder muscle fatigue using EMG based digital signal processing techniques.



**Dr. Ashish D. Nimbarte** is an Assistant Professor and the Director of Occupational Safety and Health Engineering program in the Industrial and Management Systems Engineering Department at West Virginia University. He obtained his doctorate from Louisiana State University in the interdisciplinary program of Engineering Science. His research interest is in the general area of work-related musculoskeletal disorders. Dr. Nimbarte's current research focuses on understanding the pathomechanisms of work-related neck and shoulder musculoskeletal disorders with a long term goal of developing effective control strategies.





**Majid Jaridi** is a Professor of Industrial Engineering at West Virginia University. He earned a Ph.D. from the University of Michigan in Industrial and Operations Engineering in 1983. He joined the IMSE Department at WVU in January, 1984. He has been teaching courses such as Industrial Quality Control, Quality Management, Advanced Analysis of Engineering Data, Time Series Analysis and Forecasting. In addition to his teaching and research activities, Dr. Jaridi serves as the Director of NASA West Virginia Space Grant Consortium (WVSGC) and NASA WV Experimental Program to Stimulate Competitive Research (EPSCoR). These NASA-funded programs provide support for research of interest to

NASA to faculty from WV colleges and universities, and fellowship and internship opportunities at NASA for all West Virginia students in the science, technology, engineering, and mathematics (STEM) disciplines. His research interests are in the areas of statistical quality control, forecasting and transportation planning, with which he combines his expertise in decision analysis. Dr. Jaridi has numerous journal publications and conference proceedings in the areas of quality control, decision analysis, and transportation modeling.



**Dr. Robert C. Creese** is Professor of Industrial Engineering and Graduate Program Director in the Industrial and Management Systems Engineering Department in the Benjamin M. Statler College of Engineering and Mineral Resources at West Virginia University. He obtained his BS, MS, and PhD degrees from the Pennsylvania State University(1963), the University of California-Berkeley(1964) and the Pennsylvania State University(1972). He is a life member of ASEE, AACE-International and AFS as well as a member of ASM, AWS, SME, and ICEAA. He is a registered professional engineer in Pennsylvania and West Virginia and a certified cost engineer. He has also taught at Grove City College and

The Pennsylvania State University and on sabbaticals and visits to Aalborg University in Denmark and VIT University in Vellore India. He has authored or co-authored over 100 papers and four books.